BMC Gastroenterology

RESEARCH Open Access

Diagnostic accuracy and influencing factors of microprobe endoscopic ultrasound for gastrointestinal subepithelial lesions: a multicenter retrospective study

Jiao Li[1†], Yongfeng Yan[2†], Dandan Jiang[3†], Xiaoxiang Wang[4†], Li Wang[5†], Li Liu[1], Tao Shu[1], Zhengkui Zhou[1] and Xiaobin Sun[1*]

Abstract

Background Microprobe endoscopic ultrasonography (MEUS) has been widely adopted in primary hospitals due to its affordability, ease of use, and simple operation. This study aims to assess the diagnostic accuracy of MEUS in classifying gastrointestinal subepithelial lesions (SELs), identify key influencing factors, and explore strategies for improvement.

Methods A retrospective analysis was conducted on 855 patients with histopathologically confirmed SELs across five Chinese hospitals. The overall diagnostic accuracy (DA) of MEUS for SELs was calculated. Independent factors were identified using univariate and multivariate logistic regression analyses, followed by subgroup analysis.

Results Among 896 lesions across 31 SEL types, the overall DA was 70.31%. Non-gastrointestinal stromal tumor (GIST) and non-neuroendocrine tumor (NET) lesions, along with gastric location, were identified as risk factors for lower diagnostic accuracy, while rectal location was protective. In the subgroup analysis, gastric leiomyomas had a DA of 9.85% with 99.17% incorrectly classified as GISTs, compared to 94.78% for gastric GISTs, 84.24% for gastric NETs, and 31.2% for other lesions. Lesions with inhomogeneous echoes were 20 times more likely than those with homogeneous echoes to be diagnosed as gastric GISTs compared to gastric leiomyoma. Additionally, the inhomogeneous echo patterns of gastric GISTs were characterized by hyperechogenic spots in 93.67%, marginal halos in 18.99%, and cystic changes in 13.92%.

Conclusion MEUS is effective for classifying SELs, although differentiating between gastric GISTs and leiomyomas remains challenging. Improved assessment of echo heterogeneity and expanded knowledge of atypical and rare cases may enhance diagnostic accuracy.

Keywords Endoscopic ultrasonography, Subepithelial lesions, Gastrointestinal stromal tumor

†Jiao Li, Yongfeng Yan, Dandan Jiang, Xiaoxiang Wang and Li Wang considered equally to this work.

*Correspondence:
Xiaobin Sun
xbsun1197@163.com

Full list of author information is available at the end of the article

Introduction

Subepithelial lesions (SELs) are gastrointestinal protrusions with normal overlying mucosa [1]. With increasing public health awareness and the widespread use of endoscopy, the detection rate of SELs has significantly risen to 1.6–3.4% during routine gastroscopy [2, 3]. Although most SELs are benign, some, such as gastrointestinal stromal tumors (GISTs) and neuroendocrine tumors (NETs), have malignant potential [4]. Their diverse pathology and biological behavior complicate the diagnosis, leading to unnecessary resections, repeated surveillance, patient anxiety, and healthcare burdens. Therefore, accurate diagnosis is crucial for appropriate management.

Major guidelines and expert consensus recommend endoscopic ultrasound (EUS) as the preferred method for assessing SELs [5–10]. EUS provides diagnostic value, particularly for identifying lipomas and varices [6], with an overall accuracy for SELs ranging from 64.2 to 80.1% [11–13]. However, accuracy varies by lesion types, 77–89% for GISTs [11], 50–100% for NETs [14, 15], and 37.5–82.6% for leiomyomas [11, 16], and as low as 45.5–48.0% for small gastric SELs [15]. Most existing studies are single-center, involve small sample sizes, and focus mainly on upper gastrointestinal focus.

Preoperative biopsy plays an important role in the diagnosis of SELs. The diagnostic accuracy of EUS-guided fine-needle aspiration (EUS-FNA) has been reported as 74.6% (95% CI, 69.9–78.7%), while that of EUS-guided fine-needle biopsy (EUS-FNB) is higher at 84.2% (95% CI, 80.7–87.2%) [17]. Mucosal incision-assisted biopsy (MIAB) shows even greater accuracy of 88.2% (95% CI, 84.7–91.1%) [17], and appears to outperform EUS-FNA and EUS-FNB in small SELs [18, 19]. However, these tissue acquisition techniques require specialized equipment and technical expertise, which increase healthcare costs and may carry additional risks, such as tumor seeding, metastatic spread, and procedural difficulties during subsequent endoscopic resection [7]. Consequently, their widespread use in primary care settings remains limited.

Microprobe endoscopic ultrasonography (MEUS) provides high-resolution imaging for lesion assessment [5, 6]. With increasing SEL detection rates, MEUS has been widely adopted in primary hospitals across China due to its affordability and ease of operability [20], despite limitations such as reduced performance in larger lesions, lack of Doppler capabilities, and inability to obtain tissue samples. In the absence of advanced echoendoscopes and preoperative biopsy techniques (e.g., EUS-FNA/B or MIAB) in primary hospitals, enhancing non-invasive MEUS-based diagnostic accuracy becomes a key consideration. To achieve this, it is essential to first identify the factors influencing MEUS diagnostic performance, and then explore methods to improve accuracy by analysis of these factors. For example, EUS-based T staging in gastric cancer can be influenced by ulcers, undifferentiated histology, and tumors > 2 cm [21]. However, few studies have specifically investigated factors influencing MEUS diagnostic accuracy for SELs. Therefore, this multicenter study aims to assess MEUS diagnostic accuracy in SEL classification, identify key influencing factors, and explore strategies for improvement.

Subjects and methods

Patient selection

We collected clinical and pathological data of patients with SELs who visited 5 Chinese hospital between January 2013 and December 2023 retrospectively (see Supplementary table 1s). The inclusion criteria were patients diagnosed with SELs through white light endoscopy (WLE) and MEUS, and who received a pathological diagnosis through endoscopic resection or surgical operation. The exclusion criteria were patients with non-definitive pathological diagnosis, incomplete clinical data, or diagnosed by forward-viewing or standard oblique-viewing linear echoendoscopes. The possible influencing factors affecting the diagnostic accuracy, including center, equipment, patient and lesion characteristics were collected for analysis. The upper third of the stomach is defined as the cardia and fundus, the middle third as the body, and the lower third as the antrum [22].

MEUS process

WLE was used to identify the lesions. During the MEUS examination, the water immersion method was employed, allowing water to cover the lesion and serve as a medium for ultrasound. WLE and MEUS were performed by endoscopic experts or trainees under experts' supervision at all participating hospitals, and Ultrasonic mini-probes (12/20-MHz, UM-2R/3R, Olympus, Japan; 12/20-MHz, IM-02P-202501, INNERMED, Shenzhen, China) were employed in the study (see Supplementary table 1s). A comprehensive diagnostic assessment was conducted based on multiple lesion characteristics, including lesion location, surface morphology under WLE, and MEUS-based evaluation of originating layer, echogenicity, echo heterogeneity, growth pattern, and lesion borders. These characteristics were interpreted with reference to diagnostic criteria from prior studies [23], clinical guidelines [9], and expert consensus [7, 24]. For example, a well-defined, homogeneous hypoechoic lesion in the esophagus arising from the muscularis mucosa typically suggests leiomyoma; in contrast, a gastric subepithelial lesion with heterogeneous echotexture originating from the muscularis propria is more indicative of GIST.

The MEUS reports were meticulously examined, with particular attention given to the MEUS diagnosis and the

clarity of the captured images. Key features like lesion location, size, originating layer, echogenicity, and echo heterogeneity were documented. To further analyze echo homogeneity, we retrospectively examined features like hyperechogenic spots, marginal halos, and cystic changes in gastric GISTs and leiomyomas with inhomogeneous echo patterns.

Pathological diagnosis

Most cases underwent endoscopic resection, while a few cases required surgical operation. After resection, all tissues were immediately fixed in 10% neutral formalin and routinely embedded for histological examination. Immunohistochemistry was conducted to determine the pathological diagnosis of GISTs, leiomyomas, NETs, and other SELs when necessary.

Outcomes

The study aimed to achieve three key outcomes: [1] assess the overall diagnostic accuracy of MEUS in classifying SELs [2], identify key factors influencing MEUS diagnostic accuracy, and [3] explore strategies to enhance accuracy by subgroup analysis based on these factors.

Statistical analysis

Diagnostic accuracy (DA) of MEUS refers to the proportion of cases where MEUS findings were consistent with postoperative pathological results, relative to the total number of assessments. Continuous variables with a normal distribution were reported as mean ± standard deviation and compared using Student's t-test or the Mann–Whitney U-test. Non-normally distributed continuous variables were presented as median (interquartile range) and compared with the $\chi 2$ test or Fisher's exact test. Univariate and multivariate logistic regression analyses were conducted to identify independent factors affecting the diagnostic accuracy. All statistical analyses were performed using SPSS (version 29.0), with statistical significance set at a two-tailed p-value of less than 0.05.

Results

General patient characteristics

This study initially collected data from 949 patients with pathological diagnosis. However, 94 patients undetermined by MEUS before endoscopic or surgical resection were excluded (see Supplementary Table 2s). Consequently, the study included 855 patients, with a male-to-female ratio of 1:1.29 and an average age of 53.30 ± 12.04 years. Among these patients, there were a total of 869 lesions, with an average size of 1.12 ± 0.80 cm. Postoperative pathological examination identified 31 different pathological types, including 270 cases (31.07%) of GISTs, 254 cases (29.23%) of leiomyomas, 191 cases (21.98%) of NETs, and 154 cases (17.72%) of other lesions distinct from GISTs, leiomyomas, and NETs (see Table 1 and Supplementary Table 1).

Diagnostic accuracy of MEUS and the influencing factors analysis

The overall DA of MEUS was 70.31% (611 out of 869) (see Fig. 1), with rates at individual centers ranging from 68.97 to 79.12% (see Table 1). Univariate analysis showed that older age, pathological type of leiomyoma and other lesions, lesion location in stomach, and originating layer from muscularis propria affected the diagnostic accuracy ($p < 0.05$, see Table 1). The multivariate analysis revealed that leiomyomas (OR = 0.01, 95% confidence interval (CI): 0.05 – 0.02, $p < 0.001$), other lesions (OR = 0.002, 95% CI: 0.001–0.006, $p < 0.001$), lesions located in the upper third of the stomach (OR = 0.07, 95% CI: 0.03–0.18), middle third (OR = 0.06, 95% CI: 0.02–0.14, $p < 0.001$), and lower third (OR = 0.26, 95% CI: 0.09–0.78, $p = 0.017$) were independent risk factors. Conversely, rectal lesions were an independent protective factor (OR = 1.23, 95% CI: 0.68–2.21, $p < 0.001$, see Table 1).

Subgroup analysis by pathological type and lesion location

The study indicated that both pathological type and lesion location independently affected the diagnostic accuracy of MEUS. Among 254 cases of leiomyomas, the overall DA was 47.6% (121 out of 254). For esophageal leiomyomas, the DA was 92.31% (108 out of 117), with 9 cases incorrectly classified as GISTs. In contrast, the DA for gastric leiomyomas was significantly lower at 9.85% (13 out of 132), with 99.17% (119 out of 120) incorrectly classified as GISTs. This compares to a DA of 94.78% (254 out of 268) for gastric GISTs and 84.24% (16 out of 19) for gastric NETs. These discrepancies contribute to the overall low DA in diagnosing gastric lesions. Additionally, all 5 cases of rectal leiomyomas were incorrectly classified as NETs (see Supplementary Table 3s).

Excluding GISTs, leiomyomas, and NETs, there were 154 cases across 28 different pathological types classified as other lesions, with a DA of 31.2% (48 out of 154) (see Supplementary Table 3s). For ectopic pancreas (EPs) in the stomach, the DA was 62.5% (20 out of 32); 9 cases were incorrectly classified as GISTs (see Fig. 2A), 2 as leiomyomas, and 1 as a lipoma. Lipomas had a DA of 91.3% (21 out of 23), with 1 duodenal lipoma incorrectly classified as a Brunner's gland (see Fig. 2B) and 1 rectal lipoma as a NET. All 13 stomach schwannomas were incorrectly classified: 12 as GISTs and 1 as a granular cell tumor. Cystic lesions had a DA of 10% (1 out of 10), with esophageal cysts incorrectly classified as leiomyomas and GISTs, gastric and duodenal cyst incorrectly classified as GISTs (see Fig. 2C), and rectal cysts incorrectly classified as NETs. Inflammatory fibroid polyps (IFP) in the stomach had a DA of 28.57% (2 out of 7), with 4 incorrectly

Table 1 Factors influencing the accuracy of microprobe endoscopic ultrasound in diagnosing Gastrointestinal subepithelial lesions

Variable	Number [*n* (%)]	Diagnostic accuracy [% (*n*/*n*)]	Univariable		Multivariable [a)]	
			OR (95% CI)	*P* value	OR (95% CI)	*P* value
Sex						
Male	378 (43.50)	73.54 (278/378)	1[Reference]			
Female	491 (56.50)	67.82 (333/491)	0.76 (0.56–1.02)	0.067		
Age (year)						
≤ 55	485 (55.81)	67.01 (325/485)	1 [Reference]		1 [Reference]	
>55	384 (44.19)	74.48 (286/384)	1.44 (1.07–1.93)	**0.017**[b)]	0.80 (0.49–1.31)	0.370
Center						
TPHCD	529 (60.87)	69.00 (365/529)	1[Reference]			
FPHLS	94 (10.82)	71.28 (67/94)	1.12 (0.69–1.81)	0.659		
SNCH	91 (10.47)	79.12 (72/91)	1.70 (0.99–2.92)	0.053		
FPHCD	87 (10.01)	68.97 (60/87)	0.99 (0.61–1.63)	0.995		
SCMY404	68 (7.83)	69.12 (47/68)	1.00 (0.58–1.74)	0.984		
Equipment						
Olympus	718 (82.62)	70.9 (509/718)	1[Reference]			
Innermed	151 (17.38)	67.5 (102/151)	0.86 (0.59–1.25)	0.414		
Pathological type						
GIST	270 (31.07)	94.44 (255/270)	1[Reference]		1 [Reference]	
Leiomyoma	254 (29.23)	47.64 (121/254)	0.05 (0.3 – 0.10)	**< 0.001**[b)]	0.01 (0.05 – 0.02)	**< 0.001**[b)]
NET	191 (21.98)	97.90 (187/191)	2.75 (0.90–8.42)	0.076	1.19 (0.23–6.04)	0.836
Other lesions	154 (17.72)	31.17 (48/154)	0.03 (0.01–0.05)	**< 0.001**[b)]	0.002 (0.001–0.006)	**< 0.001**[b)]
Lesion location						
Esophagus	134 (15.42)	82.09 (110/134)	1 [Reference]		1 [Reference]	
Upper third of stomach	238 (27.39)	70.59 (168/238)	0.52 (0.31–0.88)	**0.015**[b)]	0.07 (0.03–0.18)	**< 0.001**[b)]
Middle third of stomach	219 (25.20)	54.79 (120/219)	0.26 (0.16–0.44)	**< 0.001**[b)]	0.06 (0.02–0.14)	**< 0.001**[b)]
Lower third of stomach	52 (5.98)	44.23 (23/52)	0.17 (0.09–0.35)	**< 0.001**[b)]	0.26 (0.09–0.78)	**0.017**[b)]
Duodenum	6 (0.69)	66.67 (4/6)	0.44 (0.08–2.52)	0.354	0.47 (0.05–4.61)	0.518
Colon	21 (2.42)	80.95 (17/21)	0.93 (0.29-3.00)	0.900	1.15 (0.26–5.01)	0.854
Rectum	199 (22.90)	84.92 (169/199)	1.23 (0.68–2.21)	0.492	0.04 (0.01–0.16)	**< 0.001**[b)]
Size (cm)						
<2.0	747 (85.96)	70.95 (530/747)	1 [Reference]	/		
2.0–5.0	117 (13.46)	65.81 (77/117)	0.79 (0.52–1.20)	0.259		
≥5.0	5 (0.58)	80.00 (4/5)	1.64 (0.18–14.74)	0.660		
Originating layer						
Deep mucosa	75 (8.63)	81.33 (61/75)	1 [Reference]		1 [Reference]	
Muscularis mucosa	137 (15.77)	83.94 (115/137)	1.20 (0.57–2.51)	0.629	1.47(0.44–4.89)	0.527
Submucosa	212 (24.40)	75.00 (159/212)	0.69 (0.36–1.33)	0.267	3.27(0.97–11.02)	0.056
Muscularis propria	445 (51.21)	62.02 (276/445)	0.38 (0.20–0.69)	**0.002**[b)]	0.51(0.15–1.78)	0.293
Echogenicity						
Echoless	3 (0.35)	33.33 (1/3)	1 [Reference]			
Hypo-echoic	795 (91.48)	70.57 (561/795)	4.80 (0.43–53.14)	0.201		
Iso-echoic	9 (1.04)	77.78 (7/9)	7.00 (0.40-123.35)	0.184		
Hyper-echoic	49 (5.64)	75.51 (37/49)	6.17 (0.51–74.17)	0.152		
Mixed-echoic	13 (1.50)	38.46 (5/13)	1.25 (0.09–17.65)	0.869		
Echo heterogeneity[c)]						
Homogeneous	618 (78.53)	70.39 (435/618)	1[Reference]			
Inhomogeneous	169 (21.47)	70.41 (119/169)	1.00 (0.69–1.45)	0.995		

TPHCD, the Third People's Hospital of Chengdu; FPHLS, the First People's Hospital of Liangshan Yi Autonomous Prefecture; SNCH, the Suning Central Hospital; FPHCD, the First People's Hospital of Chengdu; SCMY404, Sichuan Mianyang 404 Hospital; GIST, Gastrointestinal stromal tumor; NET, Neuroendocrine tumor; CI, Confidence interval

[a)] These variables of age, pathological type, lesion location, originating layer were included in the multivariable logistic regression analysis. [b)] *P* value is statistically significant. [c)] Echo heterogeneity was not described in the original reports for 82 lesions

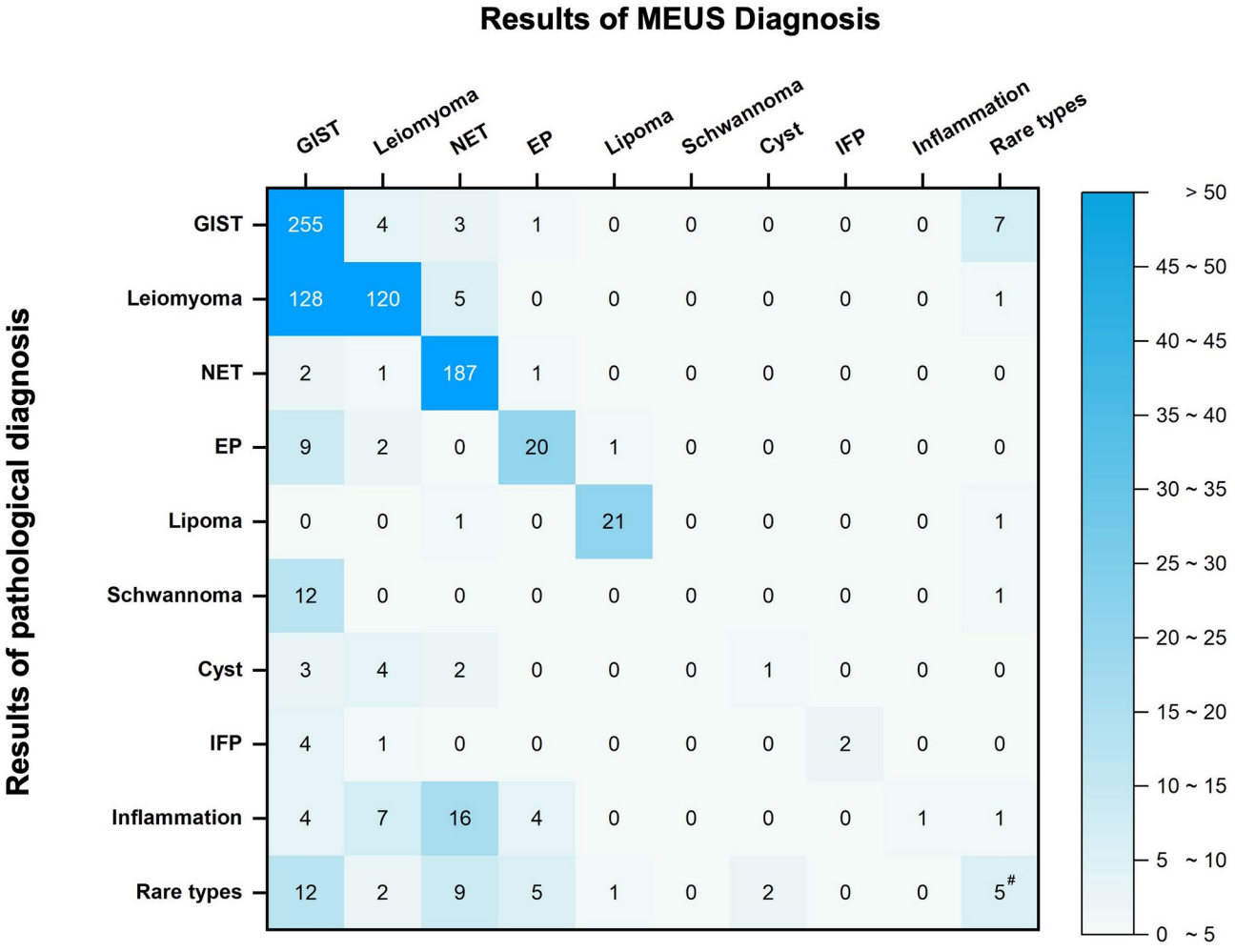

Fig. 1 Confusion matrices displaying the diagnostic result of microprobe endoscopic ultrasound compared to pathology for subepithelial lesions. Abbreviations: MEUS: Microprobe Endoscopic ultrasonography; GIST, Gastrointestinal stromal tumor; NET, Neuroendocrine tumor; EP, Ectopic pancreas; IFP, Inflammatory fibroid polyp. #, MEUS identified five rare lesion types, but only three were matched with pathological findings

classified as GISTs and 1 as a leiomyoma. Inflammatory lesions had a DA of 3.03% (1 out of 33): 8 esophageal lesions (7 incorrectly classified as leiomyomas), 10 gastric lesions (4 incorrectly classified as GISTs, 4 as EP, 1 as a collagen nodule, 1 as a NET), and 15 colorectal lesions (all incorrectly classified as NETs). Among the 36 rare lesions, only 2 cases of gastritis cystica profunda and 1 case of a Brunner's gland were correctly diagnosed. Examples of incorrectly classified cases are shown in Fig. 2D-F.

Predictive factors differentiating gastric gists from leiomyomas

Total 268 cases of gastric GISTs and 132 cases of leiomyomas were chosen for analyzed. Significant differences in clinicopathologic characteristics, including patient age, gender, lesion size, location, and echo heterogeneity, were observed between the groups ($p < 0.05$, see Supplementary Table 4s). Although both tumor types were predominantly hypoechoic, with rates of 97.01% for GISTs and 100% for leiomyomas, GISTs exhibited a significantly higher proportion of inhomogeneous echo compared to leiomyomas (31.90% vs. 1.65%, $p < 0.001$, see Supplementary Table 4).

Univariate analysis showed that GISTs were significantly associated with being male, older age, larger size, and inhomogeneous echoes. There were no significant differences in the originating layer and echogenicity between GISTs and leiomyomas. Multivariate analysis identified age over 55 years (OR = 3.05, CI: 1.86-5.00, $p < 0.001$), size of 20 mm or more (OR = 3.45, CI: 1.51–7.88, $p = 0.003$), and inhomogeneous echo (OR = 20.77, CI: 4.93–87.52, $p < 0.001$) as independent predictive factors for differentiating gastric GISTs. The middle third of the stomach (OR = 0.58, CI: 0.36–0.96, $p = 0.033$) was identified as an independent predictive factor for differentiating gastric leiomyomas (see Table 2).

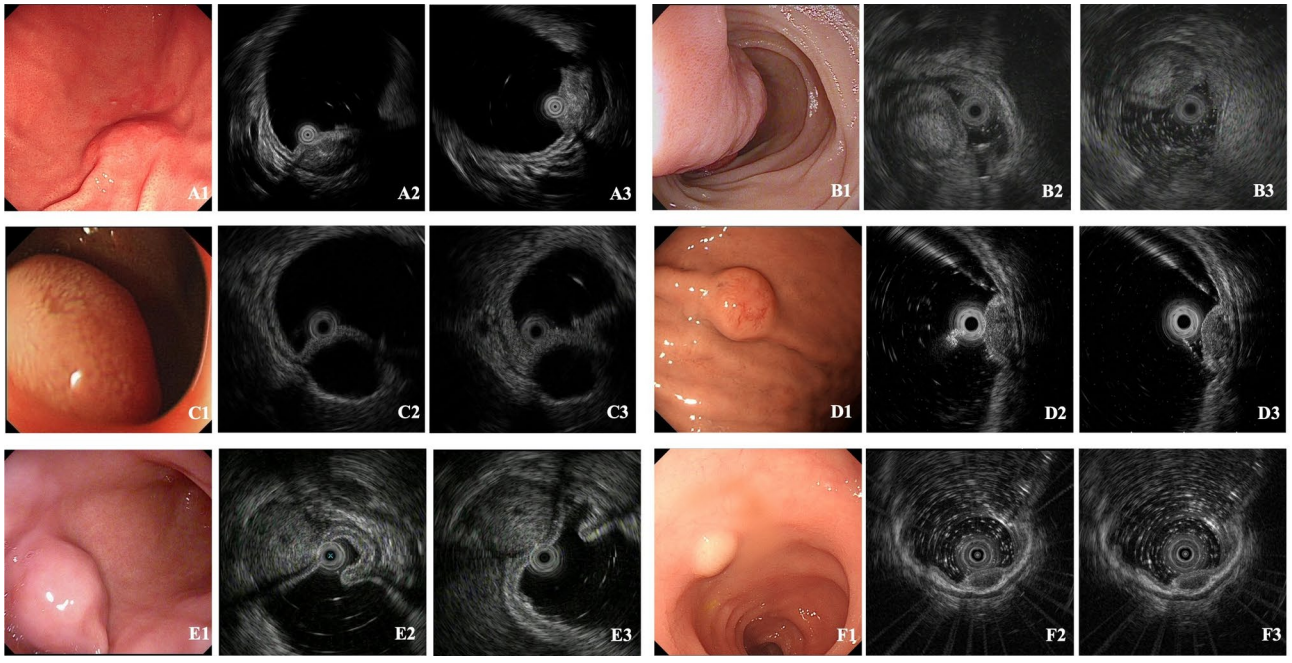

Fig. 2 Cases incorrectly classified by microprobe endoscopic ultrasonography. **A**: Gastric ectopic pancreas incorrectly classified as stromal tumor; **B**: Duodenal bulb lipoma incorrectly classified as Brunner's gland; **C**: Duodenal bulb simple cyst incorrectly classified as stromal tumor; **D**: Gastritis cystica profunda incorrectly classified as ectopic pancreas; **E**: Gastric glomus tumor incorrectly classified as stromal tumor; **F**: Rectum paraganglioma incorrectly classified as neuroendocrine tumor

The echo heterogeneity patterns in gastric gists and leiomyomas

The homogeneous echoes were present in 98.35% of gastric leiomyomas and 68.09% of gastric GISTs (Fig. 3A-B); among GISTs, lesions ≥ 2.0 cm more frequently exhibited heterogeneous echogenicity than those < 2.0 cm (42.37% vs. 29.29%), though the difference was not statistically significant ($p = 0.07$).

This analysis further examined the echo heterogeneity patterns, including 79 gastric GISTs and 2 leiomyomas with inhomogeneous echoes, excluding 3 GISTs due to missing MEUS images. Among the gastric GISTs, 93.67% (74 out of 79) displayed hyperechogenic spots, 18.99% (15 out of 79) had a marginal halo, and 13.92% (11 out of 79) showed cystic changes. Specifically, 74.68% (59 out of 79) exhibited only hyperechogenic spots (see Figs. 3C and 4A-C), 2.53% (2 out of 79) had only a marginal halo (see Fig. 3D), and 1.27% (1 out of 79) showed only cystic changes (see Fig. 3E). Additionally, 8.86% (7 out of 79) had both hyperechogenic spots and a marginal halo (see Fig. 3F), 5.06% (4 out of 79) had hyperechogenic spots with cystic changes (see Fig. 3G), 2.53% (2 out of 79) had a marginal halo with cystic changes (see Figs. 3H and 4D-G), and 5.06% (4 out of 79) exhibited all three features (see Fig. 3I). Both gastric leiomyomas showed hyperechogenic spots (100%), without of marginal halo and cystic changes. Detailed comparisons by lesion size are presented in Fig. 5 and Supplementary Table 5s.

Discussion

MEUS is increasingly adopted in primary hospitals, with an overall DA of 70.31% based on multicenter data. This study is the first to evaluate factors affecting its accuracy. Multivariate analysis identified pathological types (non-GIST and non-NET lesions) and gastric location as independent risk factors, while rectal location was a protective factor. Subgroup analysis highlighted the need to improve the identification of gastric GISTs and leiomyomas, as well as expand knowledge of atypical and rare cases. Compared to gastric leiomyoma, further analysis revealed that lesions with inhomogeneous echoes were 20 times more likely to be diagnosed as gastric GISTs than those with homogeneous echoes.

The qualitative diagnosis of SELs is fundamental for treatment and follow-up decisions. EUS plays a key role in diagnosing and managing SELs, but misdiagnosis remains a challenge [5–7]. In this study, the DA across hospitals ranged from 68.97 to 79.12%, with an overall DA of 70.31%, consistent with previous reports of 64.2–80.1% [11–13]. The exclusion of small or benign lesions not requiring resection may have contributed to the relatively lower diagnostic rate. Additionally, the study encompassed 31 different SELs from the entire gastrointestinal tract, collected from multiple hospitals, including high-altitude areas with minority populations in China, further adding diagnostic complexity. These findings

Table 2 Predictive factors for distinguishing gastric gists from leiomyomas

Variable	GIST [*n* (%)]	Leiomyoma [*n* (%)]	Univariate analysis		Multivariate analysis [a)]	
			OR (95% CI)	*P* value	OR (95% CI)	*P* value
Sex						
Male	99 (36.94)	35 (26.51)	1[Reference]		1[Reference]	
Female	169 (63.06)	97 (73.48)	0.62(0.39–0.96)	**0.039**[b)]	0.75(0.44–1.28)	0.288
Age (year)						
≤ 55	94	89	1 [Reference]		1 [Reference]	
>55	174	43	3.83(2.46–5.96)	**<0.001**[b)]	3.05(1.86-5.00)	**<0.001**[b)]
Lesion location						
Upper third of stomach	161 (60.07)	61 (46.21)	1 [Reference]		1 [Reference]	
Middle third of stomach	100 (37.31)	70 (53.03)	0.54(0.35–0.83)	**0.005**[b)]	0.58(0.36–0.96)	**0.033**[b)]
Lower third of stomach	7 (2.61)	1 (0.76)	2.65(0.32–22.01)	0.366	1.57(1.15–16.19)	0.710
Lesion size (cm)						
<2.0	208(77.61)	122(92.42)	1 [Reference]		1 [Reference]	
≥2.0	60(22.39)	10(7.58)	3.52(1.74–7.13)	**<0.001**[b)]	3.45(1.51–7.88)	**0.003**[b)]
Originating layer						
Deep mucosa	2 (0.75)	1 (0.76)	1 [Reference]			
Muscularis mucosa	1 (0.37)	2 (1.52)	0.25(0.01–7.45)	0.423		
Submucosa	12 (4.48)	4 (3.03)	1.50(0.11–21.31)	0.765		
Muscularis propria	253 (94.40)	125 (94.70)	1.01(0.09–11.27)	0.992		
Echogenicity						
Non-hypoechoic	8 (2.99)	0	1 [Reference]			
Hypo-echoic	260 (97.01)	132 (100.00)	0.00(0.00–0.00)	0.999		
Echo heterogeneity						
Homogeneous	175 (68.09) [c)]	119 (98.35) [c)]	1 [Reference]		1 [Reference]	
Inhomogeneous	82 (31.90)	2 (1.65)	27.88(6.73-115.56)	**<0.001**[b)]	20.77(4.93–87.52)	**<0.001**[b)]

GIST, Gastrointestinal stromal tumor; CI, Confidence interval

[a)] These variables of sex, age, lesion location, lesion size, and echo heterogeneity were included in the multivariable logistic regression analysis. [b)] *P* value is statistically significant. [c)] Echo heterogeneity was not described in the original reports for 11 lesions

emphasized the need for enhanced MEUS training and standardized quality control across institutions.

A key finding of this study identified leiomyoma pathology and gastric location as independent predictors of misdiagnosis with MEUS. Specifically, the DA for gastric leiomyomas was only 9.85%, with 99.17% of cases being incorrectly classified as GISTs, compared to a DA of 94.78% for gastric GISTs. This reflects the difficulty in distinguishing the small GISTs and leiomyomas, as both typically originate from the fourth or second layer and share similar EUS features, such as homogenous hypoechoic patterns, and well-defined [6]. In clinical practice, diagnostic uncertainty may lead endoscopists to favor a diagnosis of GIST to avoid the potential risk of missing malignancy, thereby contributing to the underdiagnosis of leiomyomas, as observed in our study. For larger lesions, MEUS performance may be limited by incomplete margin visualization and uncertain layer determination, warranting timely use of alternative EUS systems with superior imaging resolution. These challenges highlight the importance of improving the differentiation of gastric GISTs and leiomyomas to enhance the overall diagnostic accuracy of MEUS.

Significant differences between gastric GISTs and leiomyomas were observed in patient age, lesion size, location, and echo heterogeneity, aligning with previous studies [25–27]. Notably, GISTs have a higher incidence of inhomogeneous echoes than leiomyomas (31.90% vs. 1.65%, $p < 0.001$), with nearly 30% of lesions < 2.0 cm showing this feature. Meanwhile, lesions with inhomogeneous echoes are 20 times more likely to be diagnosed as GISTs. Age, lesion size, and location are relatively objective markers for identification, but echo heterogeneity has a much higher odds ratio, making it a critical focus for endoscopists through experience and learning. Therefore, we further analyzed the echo heterogeneity patterns of GISTs to deepen endoscopists' understanding. Hyperechogenic spots were the most common pattern, observed in 93.67% of GISTs, and pathologically correspond to calcification from tumor cell necrosis [28] (see Fig. 4A-C). The hypoechoic halo, seen in 18.99% of GISTs, indicates a pseudo-capsule formed by fibrous tissue due to tumor's expansive growth and compression of surrounding normal tissue [29](see Figs. 4D-F). Cystic changes, seen in 13.92% of GISTs, reflect necrosis or fibrous tissue [26, 30] (see Fig. 4D, E, G). In general, large, rapidly growing lesions are more prone to these

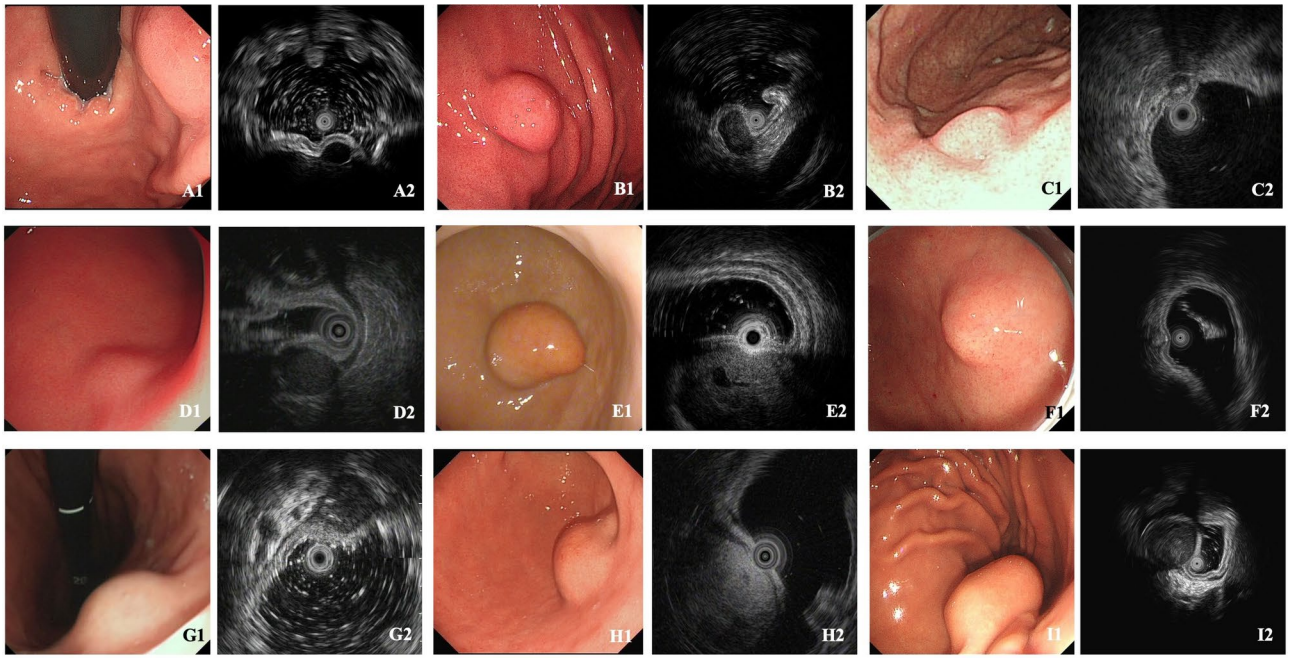

Fig. 3 Echo heterogeneity patterns of gastric gastrointestinal stromal tumor and leiomyomas. **A**: Gastric leiomyomas with homogeneous echo; **B**: Gastrointestinal stromal tumor (GIST) with homogeneous echo; **C**: GIST with hyperechogenic spots; **D**: GIST with marginal halo; **E**: GIST with cystic change; **F**: GIST with hyperechogenic spots and marginal halo; **G**: GIST with hyperechogenic spots and cystic change; **H**: GIST with marginal halo and cystic change; **I**: GIST with hyperechogenic spots, marginal halo, and cystic change

pathological changes [31]. Understanding the relationship between these EUS features and pathology can help endoscopists better distinguish GISTs from leiomyomas, improving diagnostic accuracy.

Another important result of this study was that the pathological types of lesions other than GISTs, leiomyomas, and NETs also served as independent predictors of misdiagnosis with MEUS. The DA for these lesions, including 26 different pathological types, ranged from 0 to 28.57%, with exceptions of lipomas at 91.3% and EPs at 62.5%. Incorrectly classified cases were explored in the subgroup analysis, and typical incorrectly classified cases were illustrated with images (see Fig. 2). To enhance the diagnostic accuracy of uncommon lesions, it is essential for endoscopists to continually accumulate experience and engage in ongoing education to better identify the subtle characteristics that distinguish these lesions.

In addition to the above discussed approaches, artificial intelligence-enhanced endoscopic ultrasonography (EUS-AI) approaches have demonstrated significant potential in improving diagnostic accuracy by providing an objective method to quantify the echo characteristics of SELs, making it a valuable diagnostic tool for clinicians [32–34]. In a prospective validation study, Yang X et al. [35] demonstrated that a convolutional neural network (CNN)-based AI-assisted diagnostic system significantly improved endoscopists' accuracy in distinguishing gastric GISTs from leiomyomas (78.8% vs. 69.7%). However, the diagnostic performance varies across different type of echoendoscopes, with notably lower accuracy when using mini-probes (28.6%) or radial echoendoscopes (50.0%), highlighting the need for AI models tailored specifically to MEUS systems. Similarly, in a prospective real-time clinical trial, the AI system developed by Zhixia Dong et al. [36] significantly increased the accuracy for GISTs (86.5% vs. 69.5%) and leiomyomas (86.4% vs. 69.5%), compared with endoscopists. Additionally, the AI system showed superior accuracy in diagnosing SELs measuring ≤ 20 mm compared to those larger than 20 mm (93.5% vs. 83.3%) in an external evaluation cohort [36]. Of course, EUS-AI approaches still require validation through larger-scale clinical studies and further refinement of clinical ethics before they can be fully implemented in clinical practice.

This study had several limitations. First, this study focused only on lesions with indications for MEUS examination, typically small SELs whose size precludes tissue acquisition [5]. However, this perspective highlights the diagnostic value of MEUS, especially in primary hospitals lacking advanced echoendoscopes. We hope our findings provide stronger diagnostic support for physicians relying solely on MEUS. Second, the performance of MEUS is heavily influenced by the endoscopist's skill and experience, which we could not account for. The retrospective design involved endoscopists with varying levels of experience, and their diagnostic experience varied over

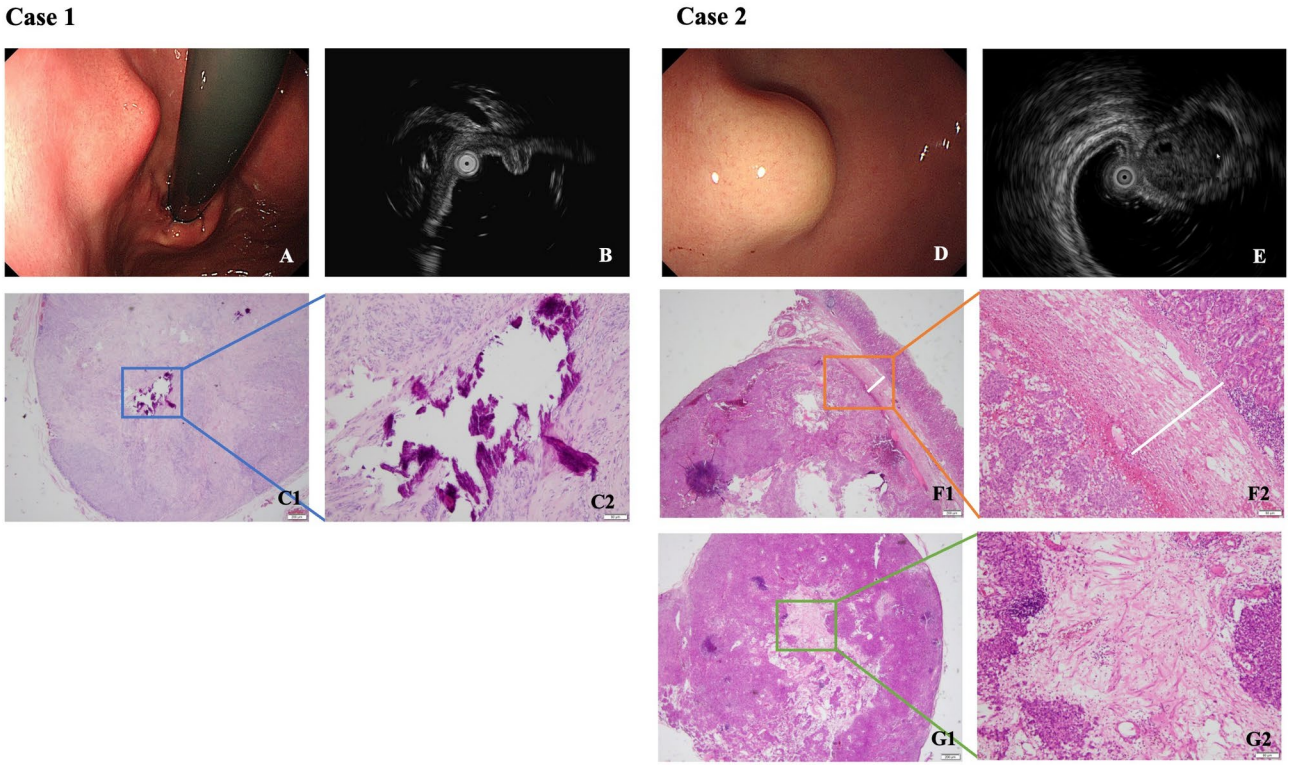

Fig. 4 Correlations between echo heterogeneity patterns with pathology in gastric gastrointestinal stromal tumors. **Case 1 A**: Endoscopy revealed a gastric body subepithelial lesion (SEL). B: MEUS identified a hypoechoic lesion with hyperechogenic spots from muscularis propria. C1-2: Histopathology confirmed intralesional calcification (C1 for HE staining x100, see blue box; C2 for HE staining x400). **Case 2D**: Endoscopy revealed a gastric fundus SEL. E: MEUS identified a hypoechoic lesion with marginal halo and cystic changes from muscularis propria. F1-2: Histopathology showed a pseudo-capsule of reactive fibrous tissue (F1 for HE staining x100, see orange box and white line; F2 for HE staining x400). G1-2: Lamellar fibrous tissue was observed (G1 for HE staining x100, see in green box; G2 for HE staining x400)

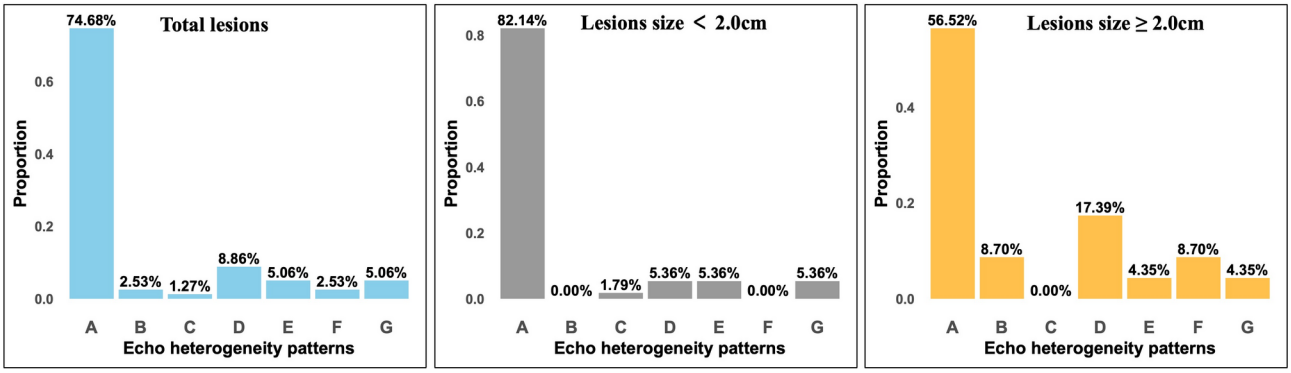

Fig. 5 Patterns of echo heterogeneity in gastric stromal tumors. **A** for hyperechogenic spots; **B** for marginal halo; **C** for cystic changes; **D** for hyperechogenic spots and marginal halo; **E** for hyperechogenic spots and cystic changes; **F** for marginal halo and cystic changes; **G** for hyperechogenic spots, marginal halo and cystic change

time, making it impossible to measure their expertise uniformly. Nevertheless, this variability may better reflect real-world practice, increasing the generalizability of our results. Third, the study included only cases with a confirmed pathological diagnosis, excluding benign lesions like EPs, lipomas, and cysts that are typically managed with follow-up. This selection may reduce the diagnostic accuracy of MEUS and introduce bias into the study population. However, identifying the malignant potential of lesions such as GISTs and NETs, which require resection or close follow-up, was the primary focus of SEL management.

Conclusion

MEUS is valuable for diagnosing SELs, although certain limitations persist. Improving diagnostic accuracy requires better recognition of echo heterogeneity patterns, such as hyperechogenic spots, hypoechoic halos, and cystic changes, particularly for differentiating gastric GISTs from leiomyomas. Greater awareness and targeted training on atypical presentations are also essential. Looking forward, AI-assisted image analysis may serve as an effective non-invasive approach to improve MEUS diagnostic performance.

Abbreviations

MEUS	Microprobe endoscopic ultrasonography
SELs	Subepithelial lesions
DA	Diagnostic accuracy
GISTs	Gastrointestinal stromal tumors
NETs	Neuroendocrine tumors
EUS	Endoscopic ultrasound
EUS-FNA	Endoscopic ultrasound -guided fine-needle aspiration or biopsy
EUS-FNB	Endoscopic ultrasound -guided fine-needle biopsy
MIAB	Mucosal incision-assisted biopsy
WLE	White light endoscopy
CI	Confidence interval
EPs	Ectopic pancreas
IFP	Inflammatory fibroid polyps
EUS-AI	Artificial intelligence-enhanced endoscopic ultrasonography
CNN	Convolutional neural network

Supplementary Information

The online version contains supplementary material available at https://doi.org/10.1186/s12876-025-03927-7.

Supplementary Material 1

Acknowledgements

None.

Author contributions

Conceptualization: Jiao Li, Xiaobin SunData curation: JL, Yongfeng Yan, Dandan Jiang, Xiaoxiang Wang, Li Wang, Li Liu, Tao Shu, Zhengkui ZhouFunding acquisition: JL, XBS, ZKZFormal analysis: JL, YFY, DDJ, XXW, LWInvestigation: JL, YFY, DDJ, XXW, LWMethodology: JL, XBSProject administration: XBSValidation: JL, XBSWriting - original draft: JLWriting - review and editing: JL, XBS.

Funding

The study was supported by the Natural Science Foundation of China (62376231), National Institute of Hospital Administration (YLXX24AIA011), the Health Commission of Sichuan Province (23LCYJ022), and the Health Commission of Chengdu (2023251, 2024070).

Data availability

Availability of data and materialsThe datasets used during the current study are available from the corresponding author on reasonable request.

Declarations

Ethics approval and consent to participate

This retrospective study was conducted in accordance with the Declaration of Helsinki and was approved by the Ethics Committee of the Third People's Hospital of Chengdu on September 21, 2023 (IRB No. 2023-S-194). Informed consent was waived due to the retrospective nature of the study, as authorized by the Ethics Committee of the Third People's Hospital of Chengdu.

Consent for publication

Not applicable.

Competing interests

The authors declare no competing interests.

Author details

[1]Department of Gastroenterology, Affiliated Hospital of Southwest Jiaotong University, The Third People's Hospital of Chengdu, Qinglong street 82#, Chengdu, Sichuan, China
[2]Department of Gastroenterology, The First People's Hospital of Liangshan Yi Autonomous Prefecture, Xichang, China
[3]Department of Gastroenterology, The Suining Central Hospital, Sunning, China
[4]Department of Gastroenterology, The First People's Hospital of Chengdu, Chengdu, China
[5]Department of Gastroenterology, Sichuan Mianyang 404 Hospital, Mianyang, China

Received: 8 February 2025 / Accepted: 22 April 2025
Published online: 09 May 2025

References

1. Sadeghi A, Zali MR, Tayefeh Norooz M, Pishgahi M, Ketabi Moghadam P. Management of Gastrointestinal subepithelial lesions: an answer to the conflicting opinions. Gastroenterol Hepatol Bed Bench. 2023;16(4):378–85.
2. Park EY, Kim GH. Diagnosis of gastric subepithelial tumors using endoscopic ultrasonography or abdominopelvic computed tomography: which is better?? Clin Endosc. 2019;52(6):519–20.
3. Choe Y, Cho YK, Kim GH, Choi JH, Kim ES, Kim JH, et al. Prevalence, natural progression, and clinical practices of upper Gastrointestinal subepithelial lesions in Korea: a multicenter study. Clin Endosc. 2023;56(6):744–53.
4. Pallio S, Crinò SF, Maida M, Sinagra E, Tripodi VF, Facciorusso A et al. Endoscopic ultrasound advanced techniques for diagnosis of Gastrointestinal stromal tumours. Cancers (Basel). 2023;15(4).
5. Jacobson BC, Bhatt A, Greer KB, Lee LS, Park WG, Sauer BG, et al. ACG clinical guideline: diagnosis and management of Gastrointestinal subepithelial lesions. Am J Gastroenterol. 2023;118(1):46–58.
6. Deprez PH, Moons LMG, O'Toole D, Gincul R, Seicean A, Pimentel-Nunes P, et al. Endoscopic management of subepithelial lesions including neuroendocrine neoplasms: European society of Gastrointestinal endoscopy (ESGE) guideline. Endoscopy. 2022;54(4):412–29.
7. Chinese consensus on endoscopic. Diagnosis and managment of Gastrointestinal submucosal tumors (version 2023). Zhonghua Shi Yong Wai Ke Za Zhi. 2023;43(3):241–51.
8. Koo DH, Ryu MH, Kim KM, Yang HK, Sawaki A, Hirota S, et al. Asian consensus guidelines for the diagnosis and management of Gastrointestinal stromal tumor. Cancer Res Treat. 2016;48(4):1155–66.
9. Faulx AL, Kothari S, Acosta RD, Agrawal D, Bruining DH, Chandrasekhara V, et al. The role of endoscopy in subepithelial lesions of the GI tract. Gastrointest Endosc. 2017;85(6):1117–32.
10. Sharzehi K, Sethi A, Savides T. AGA clinical practice update on management of subepithelial lesions encountered during routine endoscopy: expert review. Clin Gastroenterol Hepatol. 2022;20(11):2435–e434.
11. Kim SY, Shim KN, Lee JH, Lim JY, Kim TO, Choe AR, et al. Comparison of the diagnostic ability of endoscopic ultrasonography and abdominopelvic computed tomography in the diagnosis of gastric subepithelial tumors. Clin Endosc. 2019;52(6):565–73.
12. Khan S, Zhang R, Fang W, Wang T, Li S, Wang D, et al. Reliability of endoscopic ultrasound using miniprobes and grayscale histogram analysis in diagnosing upper Gastrointestinal subepithelial lesions. Gastroenterol Res Pract. 2020;2020:6591341.
13. Białek A, Wiechowska-Kozłowska A, Pertkiewicz J, Polkowski M, Milkiewicz P, Karpińska K, et al. Endoscopic submucosal dissection for treatment of gastric subepithelial tumors (with video). Gastrointest Endosc. 2012;75(2):276–86.
14. Chen HT, Xu GQ, Teng XD, Chen YP, Chen LH, Li YM. Diagnostic accuracy of endoscopic ultrasonography for rectal neuroendocrine neoplasms. World J Gastroenterol. 2014;20(30):10470–7.

15. Karaca C, Turner BG, Cizginer S, Forcione D, Brugge W. Accuracy of EUS in the evaluation of small gastric subepithelial lesions. Gastrointest Endosc. 2010;71(4):722–7.
16. He G, Wang J, Chen B, Xing X, Wang J, Chen J, et al. Feasibility of endoscopic submucosal dissection for upper Gastrointestinal submucosal tumors treatment and value of endoscopic ultrasonography in pre-operation assess and post-operation follow-up: a prospective study of 224 cases in a single medical center. Surg Endosc. 2016;30(10):4206–13.
17. Verloop CA, Goos JAC, Bruno MJ, Quispel R, van Driel L, Hol L. Diagnostic yield of endoscopic and EUS-guided biopsy techniques in subepithelial lesions of the upper GI tract: a systematic review. Gastrointest Endosc. 2024;99(6):895–e91113.
18. Facciorusso A, Crinò SF, Fugazza A, Carrara S, Spadaccini M, Colombo M, et al. Comparative diagnostic yield of different endoscopic techniques for tissue sampling of upper Gastrointestinal subepithelial lesions: a network meta-analysis. Endoscopy. 2024;56(1):31–40.
19. Dhaliwal A, Kolli S, Dhindsa BS, Devani K, Ramai D, Sayles H, et al. Clinical efficacy and safety of mucosal incision-assisted biopsy for the diagnosis of upper Gastrointestinal subepithelial tumors: A systematic review and meta-analysis. Ann Gastroenterol. 2020;33(2):155–61.
20. Liao S, Qiao W, Huang S, Yang G, Zhang R, Wu W, et al. Diagnosis of a giant gastric subepithelial lesion using a dual-frequency ultrasonic miniprobe. Endoscopy. 2023;55(S 01):E1174–5.
21. Shi D, Xi XX. Factors affecting the accuracy of endoscopic ultrasonography in the diagnosis of early gastric Cancer invasion depth: A Meta-analysis. Gastroenterol Res Pract. 2019;2019:8241381.
22. Kim TY, Yi NH, Hwang JW, Kim JH, Kim GH, Kang MS. Morphologic pattern analysis of submucosal deformities identified by endoscopic ultrasonography for predicting the depth of invasion in early gastric cancer. Surg Endosc. 2019;33(7):2169–80.
23. Alkhatib AA, Faigel DO. Endoscopic ultrasonography-guided diagnosis of subepithelial tumors. Gastrointest Endosc Clin N Am. 2012;22(2):187–205. vii.
24. Surgical Section of Chinese Society of Digestive Endoscopology. Chinese Physicians Association Endoscope Branch Digestive Endoscopy Professional Committee. Gastrointestinal surgery section of Chinese society of surgery. Chinese consensus on endoscopic diagnosis and managment of Gastrointestinal submucosal tumors (version 2018). Chin J Digestion. 2018;38(08):519–27.
25. Zhai YH, Zheng Z, Deng W, Yin J, Bai ZG, Liu XY, et al. Inflammation-related indicators to distinguish between gastric stromal tumors and leiomyomas: A retrospective study. World J Clin Cases. 2022;10(2):458–68.
26. Kim GH, Park DY, Kim S, Kim DH, Kim DH, Choi CW, et al. Is it possible to differentiate gastric gists from gastric leiomyomas by EUS? World J Gastroenterol. 2009;15(27):3376–81.
27. Kim SM, Kim EY, Cho JW, Jeon SW, Kim JH, Kim TH, et al. Predictive factors for differentiating Gastrointestinal stromal tumors from leiomyomas based on endoscopic ultrasonography findings in patients with gastric subepithelial tumors: A multicenter retrospective study. Clin Endosc. 2021;54(6):872–80.
28. Ong K, Singaporewalla RM, Tan KB. Extensive calcification within a Gastrointestinal stromal tumour: a potential diagnostic pitfall. Pathology. 2006;38(5):451–2.
29. Miettinen M, Lasota J. Gastrointestinal stromal tumors: pathology and prognosis at different sites. Semin Diagn Pathol. 2006;23(2):70–83.
30. Miettinen M, Lasota J. Gastrointestinal stromal tumors: review on morphology, molecular pathology, prognosis, and differential diagnosis. Arch Pathol Lab Med. 2006;130(10):1466–78.
31. Chen LJ, Han YD, Zhang M. CT features of calcified micro-gastric Gastrointestinal stromal tumors: a case series. BMC Med Imaging. 2023;23(1):192.
32. Ye XH, Zhao LL, Wang L. Diagnostic accuracy of endoscopic ultrasound with artificial intelligence for Gastrointestinal stromal tumors: A meta-analysis. J Dig Dis. 2022;23(5–6):253–61.
33. Gomes RSA, de Oliveira GHP, de Moura DTH, Kotinda A, Matsubayashi CO, Hirsch BS, et al. Endoscopic ultrasound artificial intelligence-assisted for prediction of Gastrointestinal stromal tumors diagnosis: A systematic review and meta-analysis. World J Gastrointest Endosc. 2023;15(8):528–39.
34. Zhang B, Zhu F, Li P, Zhu J. Artificial intelligence-assisted endoscopic ultrasound in the diagnosis of Gastrointestinal stromal tumors: a meta-analysis. Surg Endosc. 2023;37(3):1649–57.
35. Yang X, Wang H, Dong Q, Xu Y, Liu H, Ma X, et al. An artificial intelligence system for distinguishing between Gastrointestinal stromal tumors and leiomyomas using endoscopic ultrasonography. Endoscopy. 2022;54(3):251–61.
36. Dong Z, Zhao X, Zheng H, Zheng H, Chen D, Cao J, et al. Efficacy of real-time artificial intelligence-aid endoscopic ultrasonography diagnostic system in discriminating Gastrointestinal stromal tumors and leiomyomas: a multicenter diagnostic study. EClinicalMedicine. 2024;73:102656.

Publisher's note